

Protonation Effects on the Benzoxazine Formation Pathways and Products Distribution

Francisco W. M. Ribeiro,^[a, b] Isaac Omari,^[a] J. Scott McIndoe,^[a] and Thiago C. Correra^{*[b]}

The effect of acidic media on the formation of the 3,4-dihydro-2H-3-phenyl-1,3-benzoxazine **Bz** is evaluated, focusing on the differentiation of intermediates and products formed by the distinct pathways observed in the presence and absence of acid. The use of real-time mass spectrometry (PSI-ESI-MS) coupled to *tandem* mass spectrometry and infrared multiple photon dissociation (IRMPD) allowed the differentiation of the species observed during the synthesis of benzoxazines in these different conditions. The results suggest that formic acid promotes the formation of aniline and phenol condensation

products (**IC** and **IIC**) by protecting the aniline amino group and enhancing the formaldehyde electrophilicity. The results also suggest that although the presence of acid allow a more efficient potential energy landscape to be accessed, the last cyclization step for the formation of benzoxazines cannot be mediated by the protonation route intermediate (**ROP Bz**). Overall, the conclusions presented here provide important information about the synthesis of benzoxazines under acidic conditions, allowing the development of optimal reaction conditions.

Introduction

Benzoxazines are a class of easily prepared heterocyclic compounds that consist of an oxazine ring fused to a benzene ring.^[1–3] The polybenzoxazines resins formed by the polymerization of the benzoxazine monomers have been explored as a low-cost alternative for common petroleum-based resins.^[1,4–6] Accordingly, new methods, synthetic strategies and source materials for novel benzoxazine precursors have become sought after. The advances in this area can be witnessed by reports describing the use of polybenzoxazines produced from different source materials and by diverse strategies as bioactive polymers, superhydrophobic materials, anti-corrosion coatings, shape memory and self-healing materials, in electrochromic, environmental and textile applications.^[7–13] This variety of applications is based on the fact that benzoxazines can be tailored for different uses by employing distinct reactants, additives and reaction conditions, allowing the resin properties to be adjusted.^[14]

Despite their simple synthesis from a phenolic compound with unprotected *ortho* positions, a primary amine and formaldehyde, some benzoxazines poses an increased synthetic challenge due to substituent effects and the specific reactivity of the actual reactants used.^[15–17] In this context, the development of different reaction conditions and the understanding of

factors that influence the reaction outcome become instrumental for the production of specific polybenzoxazines.

Different solvents, reaction temperatures and other conditions were previously evaluated and showed great effect on the reaction outcome.^[1,6] The ideal temperature for the production of benzoxazine monomer, for instance, was determined to be around 80 °C.^[18] However, some reactants and products can undergo oxidation at higher temperatures, generating species that can influence the benzoxazine formation.^[19,20]

The use of acids was also reported in literature to improve the yield of benzoxazines.^[21,22] Aversa *et al.* reported the synthesis of 3,4-dihydro-6,8-dimethyl-2H-3-phenyl-1,3-benzoxazine **3** at room temperature from *N*-(2-hydroxy-3,5-dimethylbenzyl)- β -aminopropanoic acid **2** (Figure 1b) using ethanol as solvent in the presence of sulfuric acid.^[21] This approach allowed the reaction to be carried out at much lower temperature than the original methodology presented by Burke *et al.*, which involved heating the reaction media under 1,4-dioxane reflux at 101 °C (Figure 1a).

Some 3,4-dihydro-2H-1,3-benzoxazines with substituents on methylene carbons (oxazine ring, *sp*³ carbons) such as 2,2-dibenz-1,3-oxazine, were also synthesized by the reactions of salicylamines (o-hydroxybenzylamine) with glyoxal or diketones in methanol at lower temperatures (20 °C).^[23]

3,4-dihydro-2H-1,3-benzoxazines **Bz** were also synthesized in one-pot by directed *ortho*-lithiation of phenols and by sidechain lithiation of substituted phenols in the presence of *N,N*-bis[(benzotriazol-1-yl) methyl] amines (Figure 1c).^[24]

Another display that the reaction conditions have a great impact in the benzoxazine preparation is reported by Oliveira *et al.* They report the formaldehyde-free synthesis of a cardanol **4** biobased benzoxazine using microwave radiation and hexamethylenetetramine (HMTA) in few minutes (Figure 1d).^[25]

Deng *et al.* reported a kinetic study on the formation of 3,4-dihydro-2H-3-phenyl-1,3-benzoxazine **Bz** (Figure 1e) and found

[a] F. W. M. Ribeiro, I. Omari, J. Scott McIndoe
Department of Chemistry, University of Victoria, P. O. Box 3065, Victoria, BC
V8W 3V6, Canada

[b] F. W. M. Ribeiro, T. C. Correra
Department of Fundamental Chemistry, Institute of Chemistry, University of
São Paulo Av. Prof. Lineu Prestes, 748, Cidade Universitária, São Paulo, São
Paulo, 05508-000, Brazil,
E-mail: tcorrera@iq.usp.br

Supporting information for this article is available on the WWW under
<https://doi.org/10.1002/cphc.202400295>

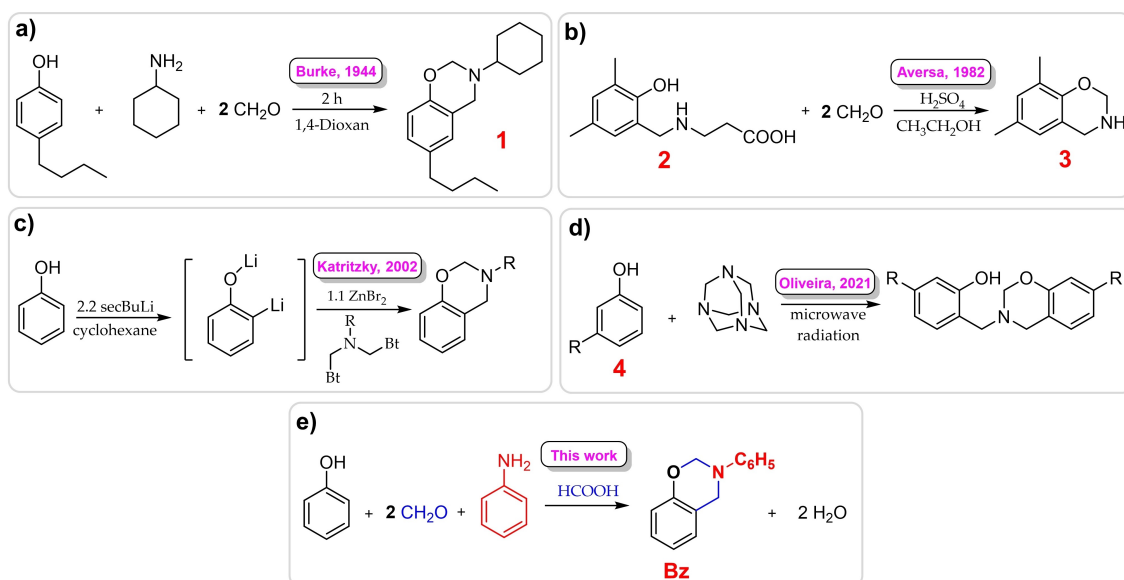


Figure 1. Diverse approaches for the benzoxazines synthesis: a) traditional method for the synthesis of benzoxazine using 1,4-Dioxan reflux (101 °C), b) condensation using sulfuric acid at room temperature, c) benzoxazine synthesis using organolithium compounds at 80 °C, d) formaldehyde-free benzoxazine synthesis from cardanol (R represents the 4 different alkyl chains and different insaturations) and e) synthesis of 3,4-dihydro-2H-3-phenyl-1,3-benzoxazine **Bz** in the presence of formic acid (0.1 % in volume) evaluated in this work.

that the concentration of benzoxazine during the reaction is consistent with an acid-catalyzed methylene glycol dehydration being the rate-controlling step in the overall reaction between a Mannich base and formaldehyde to form benzoxazine.^[26]

Thus, the presence of an acid in the reaction media play an important role in the production of benzoxazine monomers.^[27] This is expected because the formation of the imine/iminium intermediates involved in this process was previously shown to be pH-dependent.^[28]

In this context, this study evaluated the formation of 3,4-dihydro-2H-1,3-benzoxazine **Bz** from phenol, formaldehyde and aniline in the presence and absence of formic acid as the proton source by following the reaction in real time by mass spectrometry. The ion structure for the species observed to be present at the reaction media was further evaluated by tandem MS, infrared multiple photon dissociation (IRMPD) spectroscopy and theoretical modeling using density functional theory (DFT) calculations so the effect of the acid medium in the reaction pathways could be unraveled.

Methodology

The 3,4-dihydro-2H-3-phenyl-1,3-benzoxazine **Bz** synthesis was carried out by adding 0.18 mmol of phenol (Sigma, ≥ 99.5%) and aniline 0.18 mmol (Sigma, ≥ 99.5%) to a reaction flask containing 6.0 mL of CH₃CN (Sigma, ≥ 99.5%).^[2,29] The effect of the acidic media was evaluated by adding 1.0 mL of 0.1 % formic acid to the 10 mL of CH₃CN before the addition of the other reactants resulting in a final formic acid concentration of 0.01 %. After the complete dilution of the phenol and aniline, 0.37 mmol of formaldehyde (Sigma, 37%) was added and the mixture was stirred for 1.0 hour at 353 K.^[1,2]

The reaction was examined by a triple quadrupole mass spectrometer (Waters Acquity Triple Quadrupole Detector-TQD). The reactions were sampled in real time by the ESI-PSI (Electrospray ionization – pressurized sample infusion)^[30–32] method. In this method, a reaction vessel was pressurized with 5 psi of N₂ and the reaction media was transferred to the ESI source via PEEK tubing at an estimated flow rate of 40 μL/min. The MS parameters used were as follows: capillary voltage 3.0 kV; cone voltage 15 V; extraction voltage 3.0 V; temperature source 90 °C; cone gas flow rate 100 μL/h; desolvation gas flow rate: 100 L/h, number of scans 5. Collision-induced dissociation (CID) experiments were carried out with argon (99.999%) and the excitation energy in the 5 to 40 V range.^[33,34] CID spectra are available in Figure S1.

IRMPD spectra for the relevant species (Figure S2 and S3) were recorded in the 2800–3800 cm⁻¹ range by coupling an optical parametric oscillator/amplifier (OPO/OPA; LaserVision 14–21 mJ/pulse, 3.7 cm⁻¹ resolution) output beam to an in-house modified 3D ion trap described previously.^[35] The photo-fragmentation efficiency at a given wavelength ν , PE ν , was calculated according to the equation $PE\nu = -\ln((P\nu)/(P\nu + \Sigma Pj\nu))$, where $P\nu$ represents the parent ion intensity at a given wavelength; ν and $Pj\nu$ represent the fragment ion intensities at the same wavelength ν . The laser beam power dependence with the wavenumber can be found in the Supporting Information (Figure S4).

All quantum mechanical calculations were carried out using Gaussian 09 (Revision C.01)^[36] employing the B3LYP functional^[37] for optimizations at the 6–311++G(d,p)^[38] basis set with default convergence criteria. The suitability of this methodology is discussed elsewhere.^[39,40]

The vibrational analysis showed the absence of imaginary frequencies for all stationary points along the potential energy

surfaces with exception of the transition states, that showed one imaginary frequency confirmed by intrinsic reaction coordinates (IRC) calculations to be correlated to the TS found.^[36] Vibrational analysis was also compared with the experimental IRMPD spectra by using a scale factor of 0.967.^[41] Solvation effects were included in all single point calculations with the polarizable continuum model (PCM),^[42] considering CH₃CN as solvent. All reported energy values are reported as relative Gibbs energy in kJ.mol⁻¹ at 353.15 K. The coordinates for the structures presented in this work are available in the Supplementary Information.

Results and Discussion

Experimental Results

To evaluate the effect of the acidic media on the benzoxazine synthesis, the reaction media of a mixture of aniline, formaldehyde and phenol were evaluated by PSI-ESI(+)-MS.

Figure 2a shows a typical mass spectrum obtained for the reaction media after the reaction is completed using CH₃CN as solvent in the absence of any acid addition. Figure 2b shows the mass spectrum for this same sample used in Figure 2a with 0.01% of formic acid added just before the MS analysis, and Figure 2c shows a mass spectrum during the online reaction in acetonitrile with formic acid (0.01%) added at the beginning of the reaction.

The reaction in absence of formic acid (Figure 2a) shows signals assigned as the protonated aniline with m/z 94 and the iminium intermediate and some isomeric side products with m/z 106, as observed in previous reports.^[2,43] The species were

observed in low intensities under these reaction conditions as can be derived by the presence of contaminants that would not be observed in the presence of high ion counts as, for instance, the species with m/z 105 assigned as the $[(\text{CH}_3\text{CN})_2 + \text{Na}]^+$ cluster.

It is known that ESI-MS analysis can be influenced by the addition of acids and other additives^[44,45] and this effect was evaluated in Figure 2b. The addition of acid to the same solution evaluated in Figure 2a immediately before the analysis allows the detection of the intermediate with m/z 124 – the species **Ia**, precursor of the iminium ion **IIa**, in addition to the protonated intermediate **III** with m/z 200 generated by the reaction between phenol and imine, besides the protonated benzoxazine product **Bz** with m/z 212.

Figure 2c show the same reaction carried out in the presence of 0.01% formic acid from the beginning of the reaction. In addition to the characteristic intermediates and **[Bz + H]⁺** observed in Figure 2b, species with m/z 209 (**IIc**) and m/z 315 (**Ic**) were also observed.^[46,47] The nature of these species will be discussed further on the text.

By comparing Figure 2b to Figure 2c, it is possible to rule out that the acid presence could have enhanced the ionization efficiency of the species **IIc** and **Ic** that could be present in the absence of acid. Therefore, these results suggest the use of acid since the beginning of the reaction does interfere with the reaction mechanism. A better evaluation of the progress of the reaction media during the reaction can be obtained by the real-time analysis of the reaction media in both conditions (with and without acid) shown in Figure 2(d–e), respectively.

Figure 2(d–e) shows that, in both conditions, the intensity of aniline (m/z 94, red) decreases dramatically after 30 min as expected by the consumption of aniline to form the product.

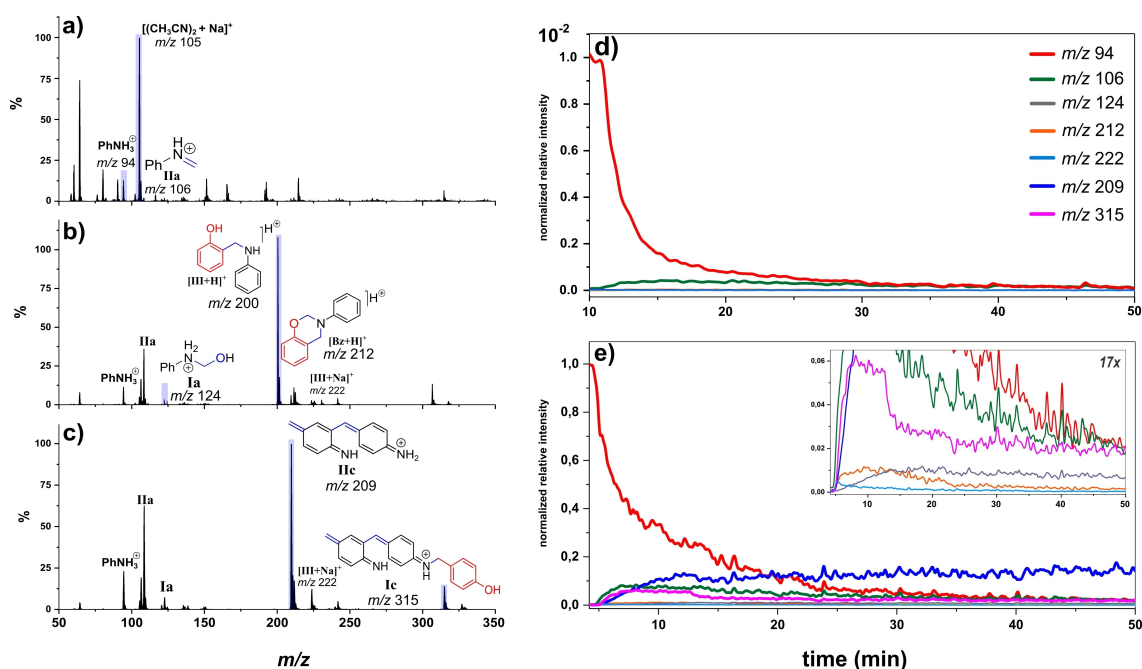


Figure 2. Mass spectra for the benzoxazine **Bz** synthesis: a) without acid addition, b) with addition of formic acid just before the MS analysis and c) with formic acid addition since the beginning of the reaction. Real-time analysis by PSI-ESI(+)-MS of **Bz** synthesis in the d) absence and e) presence of formic acid.

For the reaction carried out without acid addition, only the intermediate with m/z 106 (**IIa**) can be observed reaching its maximum intensity after 15 min. After 30 min no significant changes to the ion intensities were observed. Only trace amounts of the ions with m/z 209 and 315 (**IIc** and **Ic**) are observed in these conditions.

The reaction in acidic media shows signals relative to the intermediates with m/z 106, and intermediates with m/z 124 (**Ia**) besides the protonated product as m/z 212 and the sodiated intermediate **III** as m/z 222 in trace amounts after two minutes. The by-products **IIc** and **Ic** are observed in considerable intensities (10× the **Bz** product) being formed up to 12 min. After that, the intensity of **IIc** increases slowly. The by-product **Ic** decreases steadily after this period accompanied by a decrease in the $[\text{Bz} + \text{H}]^+$ intensity, suggesting that **Ic** can be subjected to further reactions, as already observed for **Bz**.^[48]

Side Products Observed in the Presence of Acidic Media

The ion with m/z 209 was assigned as **IIc** based on previous reports from Crescentini *et al.* that observed **IIc** species to be present during the analysis of commercial methylenedianiline (MDA) using ion mobility spectrometry.^[46,47]

The formation of compound **IIc** can be explained by the reaction of aniline and formaldehyde followed by a dehydration to form the intermediate **D** (Figure 3a) previously observed by our group.^[43] Two molecules of this intermediate **D** can react to form compound **IIc** (Figure 3a). Although it is possible that **IIc** (and **Ic**) could react with additional **D** molecules, no higher molecular mass species were observed in this study.

IIc could react with another formaldehyde molecule generating the intermediate **E** after dehydration (Figure 3b) that would be prone to a phenol attack generating **Ic**. The identity of both species, **IIc** and **Ic**, were confirmed by tandem MS (Figure S1) and IRMPD spectroscopy (Figures S2 and S3).

We suggest that the species **Ic** and **IIc** are formed in the presence of acid for two reasons: i) the protonation of the aniline amino group reduces its nucleophilicity towards the formaldehyde to start the benzoxazine formation via the

intermediates **Ia** or **Ib** and; ii) the protonation of the formaldehyde increases its electrophilicity allowing the aromatic attack depicted in Figure 3b. It is important to highlight that this hypothesis would be in accordance with the fact that only trace amounts of **Ic** and **IIc** were observed in the reaction media carried out without acid addition.

The greater reactivity of the aromatic ring promoted by the aniline protonation could enable reactions to take place in the *ortho*, *meta* and *para* positions, adding further variability to these subproducts.^[46]

Benzoxazine Formation Mechanism in Acidic Media

To rationalize the different species generated under acidic conditions, the following mechanism is proposed [Figure 4(a–b)], based not only on the species observed but also on previous works of Ishida's and Ribeiro's.^[1,2]

Our proposal is that in the initial step the primary amine (aniline) will react with formaldehyde to form either the protonated (Figure 4a) or the neutral (Figure 4b) N-hydroxymethyl amine intermediate **I**, observed as the ion with m/z 124.

In the presence of an acidic media, the dehydration of intermediate **Ia** would give rise to the imine intermediate (**IIa**). This electrophilic species would be susceptible to an electrophilic aromatic substitution with the phenol ring, forming intermediate **III** that would react with another formaldehyde molecule forming **IVa**. This species would later undergo dehydration to generate **ROP-Bz**, which could form the benzoxazines **Bz**, depending on the transition state viability, as will be discussed further on. The nomenclature **ROP-Bz** is used in this case as this is the same intermediate for the ring opening polymerization of the **Bz** previously characterized.^[48]

Without the addition of acid to the reaction media, the mechanism would take place via the imine **IIb** that, in a similar fashion, would be prone to an electrophilic aromatic substitution to form intermediate **III** after proton transfer. A further attack to another formaldehyde molecule would yield the intermediate **IVb** that would dehydrate to form the benzoxazines monomer in its neutral form (Figure 4b).

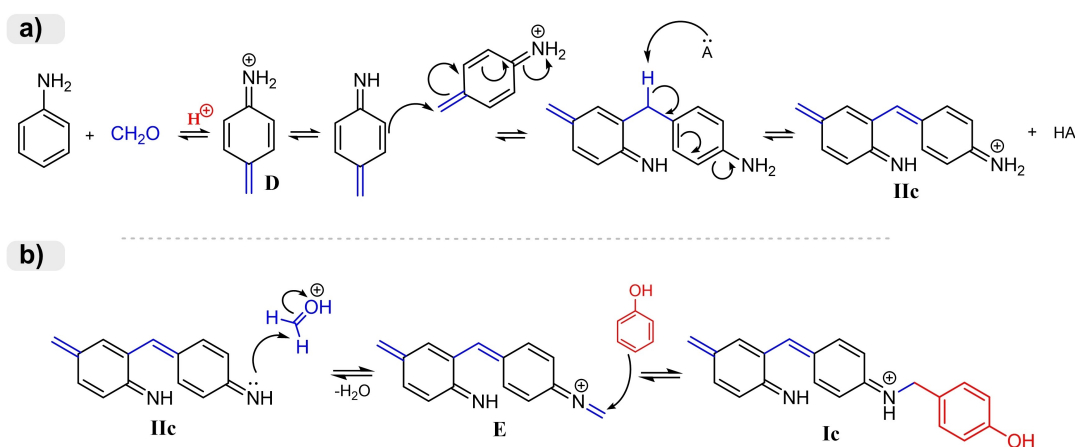


Figure 3. a) Mechanism of synthesis of the compound **IIc**, b) Synthesis of compound **Ic** from **IIc**.

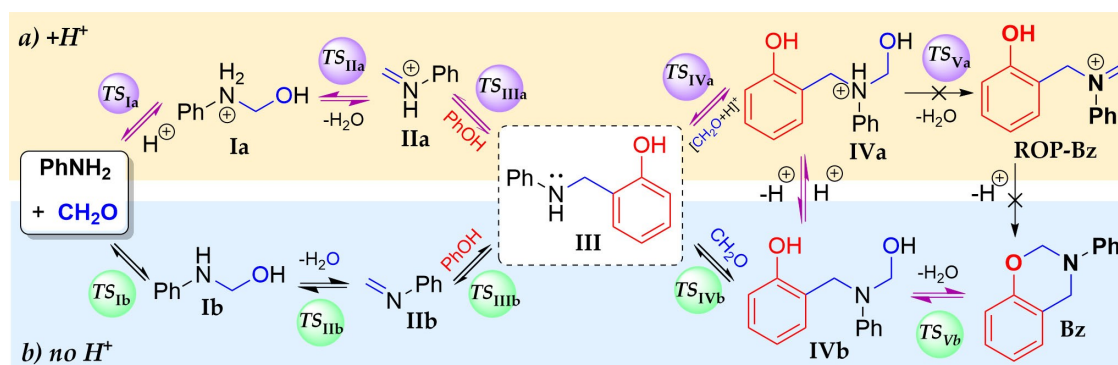


Figure 4. Different reaction pathways proposed for the benzoxazine formation a) with acid addition and b) without acid addition. The purple arrow indicates the overall path to the formation of Bz.

These reaction mechanisms were modeled by electronic structure calculations (Figure 5) so the reaction thermochemistry and, therefore, the mechanism viability, could be evaluated.

Figure 5a and 5b show the potential energy surface for the proposed mechanisms with and without the use of acid, respectively. The overall exergonicity in the presence of acid ($127.8 \text{ kJ mol}^{-1}$) is greatly reduced to 4.3 kJ mol^{-1} without acid.

This would be in line with the fact that the acid presence is extremely relevant for the formation of the iminium **IIa** ion (Figure 5) as there is an ideal pH range of 4–6^[49] that must be present in order to protonate the formaldehyde carbonyl and avoid the protonation of the amine group. This effect can be observed in Figure 5 as the transition state **TSIIa** for the formation of the iminium **IIa** in the presence of a proton is 195.3 kJ/mol lower in energy than the **TSIIb** for the same process in the absence of an acid (Figure 5).

It is interesting to notice that despite the mechanism representing the acid effect has most of the transition states

and intermediates lower in energy than the mechanism without acid, the Gibbs energy of the **TSVa** transition state representing the dehydration step to generate the **ROP-Bz** intermediate is 240 kJ mol^{-1} higher than the isolated reactants. Therefore, this last step would not be kinetically favored relatively to the neutral one, which is $131.4 \text{ kJ mol}^{-1}$ lower in energy.

This observation suggests that the acid pathway is the most favorable path up to the intermediate **IVa**. In this point the protonation equilibrium favors the neutral **IVb** intermediate by 28.3 kJ mol^{-1} , and this **IVb** intermediate would proceed to the final dehydration to form the benzoxazine product **Bz**.

So, the formation of benzoxazines is proposed to be dependent on the presence of acid or acidic reagents up to the last dehydration step, that takes place via the unprotonated intermediate **IVb** to produce the benzoxazine species.

Figure 6 represents the final steps of the benzoxazines cyclization process in detail. In blue, the cyclization of the

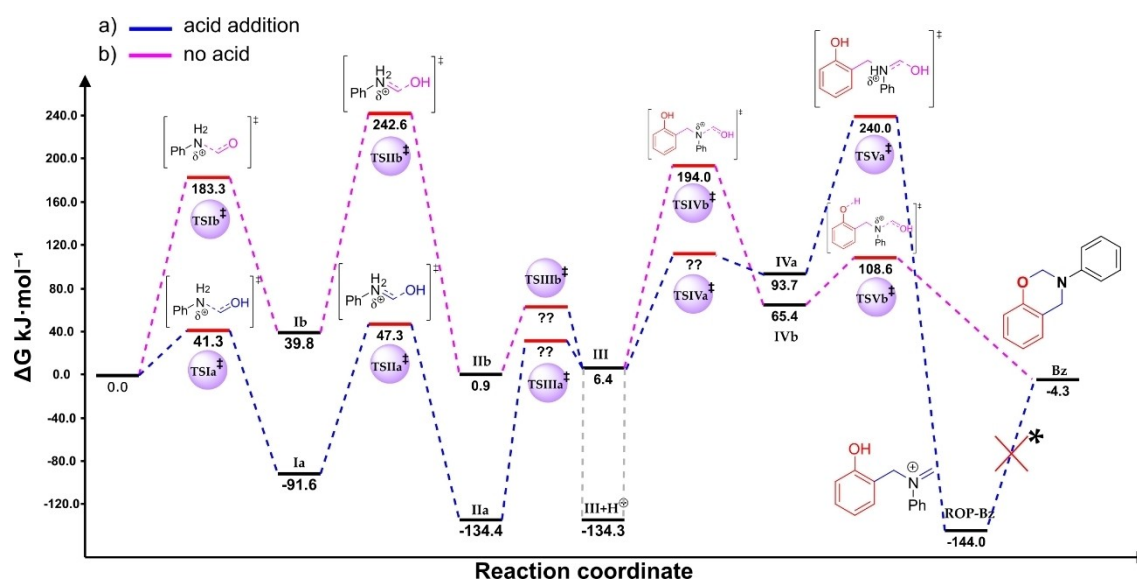


Figure 5. Potential energy surface for the benzoxazine **Bz** synthesis at the B3LYP/6-311++G(d,p) level of theory considering acetonitrile as solvent (PCM): a) in the presence and, b) absence of acid. Energy for the protonated intermediate **III** (**III**+H⁺) is shown for reference. Transition states with question marks denotes species that were not found.*A detailed description of the last reaction step is presented in Figure 6.

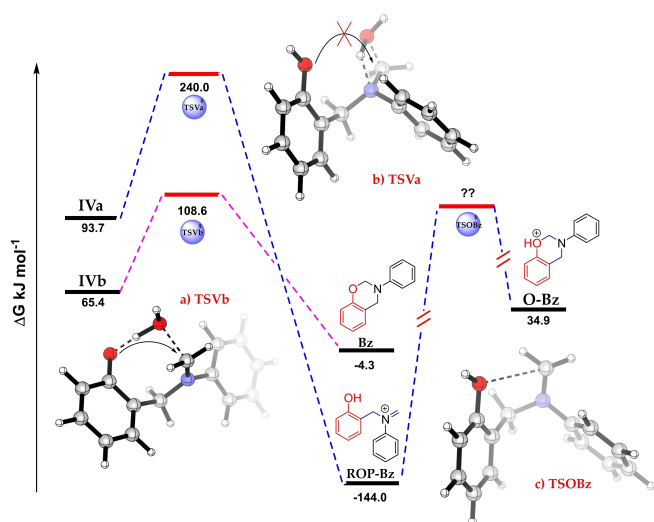


Figure 6. Final steps of the potential energy surface for the benzoxazine **Bz** synthesis at the B3LYP/6-311++G(d,p) level of theory considering acetonitrile as solvent (PCM) a) in the presence (blue) and, b) absence (pink) of acid.

protonated benzoxazine monomer can be seen, while in pink the process for the unprotonated species is depicted.

Besides the fact that the TS for the neutral pathway is more favorable by $131.4 \text{ kJ mol}^{-1}$ than the protonated pathway, as discussed in Figure 5, a careful evaluation shows that while the neutral pathway would lead directly to the benzoxazine via **TSVb**, the protonated pathway leads to the iminium intermediate **ROP Bz**.

This path occurs because the **TSVb** for the neutral pathway allows the intramolecular dehydration to take place concerted with attack on the adjacent electrophilic carbon, allowing the ring formation to produce **Bz** to take place (Figure 6a). The protonated species cannot perform these processes in a concerted way and the dehydration generates the iminium intermediate **ROP Bz** (Figure 6b).

Even with the **ROP Bz** formation being less favorable, the literature describes this species as the intermediate that allows the formation of benzoxazine.^[50] Nevertheless, we have previously described that the **Bz** protonated at the oxygen atom (**O-Bz**) that would be formed upon cyclization of **ROP Bz** is not a stable species.^[2,51]

In fact, our calculations show that upon protonation of the benzoxazines at the O center, the species spontaneously break and forms the **ROP Bz** species. This result is in line with the fact that the TS for the cyclization of **ROP Bz** could not be found, suggesting barrier to form **O-Bz** from **ROP Bz** (**TSOBz**) is inaccessible, as the reverse pathway seems to be spontaneous and have $178.9 \text{ kJ mol}^{-1}$ of relative Gibbs energy as driving force.

Conclusions

This work studied the role of the acidic medium in the formation of benzoxazine by evaluating the reaction intermedi-

ates and products observed by mass spectrometry. Possible reaction mechanisms were further examined by DFT calculations. The experimental results show that the addition of formic acid promotes the formation of aniline and phenol condensation subproducts **Ic** and **IIc**, as characterized by mass spectrometry, and monitored over time using PSI-ESI-MS and confirmed by tandem MS and IRMPD spectroscopy.

The potential energy surface calculated at B3LYP/6-311++G(d,p) and PCM solvation model show that the protonated pathway is favored over the neutral pathway up to the last reaction step for the cyclization and formation of the benzoxazine. At this stage the formation of the **ROP Bz** iminium intermediate dehydration (**ROP Bz**) would not be favorable. Conversely, the neutral pathway at this stage would form the benzoxazine **Bz** directly by dehydration and cyclization via a concerted TS that is $131.4 \text{ kJ mol}^{-1}$ lower in energy than the protonated pathway.

The formation of species **Ic** and **IIc** under acidic conditions can be explained by the protonation of the aniline amine group and the formaldehyde, making the aromatic attack to the formaldehyde a favorable pathway in the presence of acid.

Acknowledgements

The authors would like to acknowledge The Sao Paulo Research Foundation (FAPESP grants 2014/15962-5, 2015/08539-1, 2019/25634-9, 2021/06726-0, 2022/00498-8) and the Coordination for the Improvement of Higher Education (CAPES Finance code 001 and grant 23038.006960/2014-65) for substantial support for the current research. F.W.M.R. would like to thank FAPESP for the fellowships (2017/18485-1, 2019/16026-5, and 2023/01180-4) and T.C.C. would like to thank the National Council for Scientific and Technological Development (CNPq) for the fellowship 305858/2020-3 and 306701/2023-5.

Conflict of Interests

The authors declare no conflict of interest.

Data Availability Statement

The data that support the findings of this study are available from the corresponding author upon reasonable request.

Keywords: Acid Catalysis · Benzoxazines · Polybenzoxazines · Mass Spectrometry · Reaction Mechanism

- [1] H. Ishida, T. Agag, Eds. *Handbook of Benzoxazine Resins* Elsevier, **2011**. <https://doi.org/10.1016/C2010-0-66598-9>.
- [2] F. W. M. Ribeiro, A. F. Rodrigues-Oliveira, T. C. Correra, *J. Phys. Chem. A* **2019**, *123*(38), 8179–8187. <https://doi.org/10.1021/acs.jpca.9b05065>.
- [3] B. Lochab, M. Monisha, N. Amarnath, P. Sharma, S. Mukherjee, H. Ishida, *Polymers (Basel)*. **2021**, *13*(8), 1260. <https://doi.org/10.3390/polym13081260>.

- [4] P. Froimowicz, K. Zhang, H. Ishida, *Chem. A Eur. J.* **2016**, 22(8), 2691–2707. <https://doi.org/10.1002/chem.201503477>.
- [5] M. L. Salum, D. Iguchi, C. R. Arza, L. Han, H. Ishida, P. Froimowicz, *ACS Sustainable Chem. Eng.* **2018**, 6(10), 13096–13106. <https://doi.org/10.1021/acssuschemeng.8b02641>.
- [6] H. Ishida, P. Froimowicz, *Advanced and Emerging Polybenzoxazine Science and Technology* Elsevier, **2017**. <https://doi.org/10.1016/B978-0-12-804170-3.09987-X>.
- [7] F. W. Holly, A. C. Cope, *J. Am. Chem. Soc.* **1944**, 66(11), 1875–1879. <https://doi.org/10.1021/ja01239a022>.
- [8] Yuan Liu, Yunyan Peng, Jun Luo, Jingkai Liu, X. L. Synthesis, *Ind. Eng. Chem. Res.* **2020**, 59(26), 12085–12095. <https://doi.org/10.1038/s41598-023-30364-x>.
- [9] Yuan Liu, Yunyan Peng, Jun Luo, Jingkai Liu, X. L. Adsorption, *Ind. Eng. Chem. Res.* **2020**, 59(26), 12085–12095. <https://doi.org/doi.org/10.1021/acssuschemeng.9b04163>.
- [10] L. R. de Souza, J. R. M. D'Almeida, X. Cheng, L.-H. Rong, E. B. Caldona, R. C. Advincula, *Mater. Today Commun.* **2022**, 30, 102988. <https://doi.org/10.1016/j.mtcomm.2021.102988>.
- [11] A. Jamrozik, M. Barczewski, G. Framski, D. Baranowski, P. Jakubowska, Ł. Klapiszewski, T. Jesionowski, A. Voelkel, B. Strzemiescka, *Materials (Basel)* **2020**, 13(13), 2995. <https://doi.org/10.3390/ma13132995>.
- [12] Z. Shen, Y. Liu, J. Li, L. Xu, G. Liu, *High Perform. Polym.* **2020**, 32(10), 1122–1130. <https://doi.org/10.1177/0954008320933659>.
- [13] Y. Liu, R. Yin, X. Yu, K. Zhang, *Macromol. Chem. Phys.* **2019**, 220(1), 1–7. <https://doi.org/10.1002/macp.201800291>.
- [14] M. L. Salum, D. Iguchi, C. R. Arza, L. Han, H. Ishida, P. Froimowicz, *ACS Sustainable Chem. Eng.* **2018**, 6(10), 13096–13106. <https://doi.org/10.1021/acssuschemeng.8b02641>.
- [15] T. Agag, L. Jin, H. Ishida, *Polymer* **2009**, 50(25), 5940–5944. <https://doi.org/10.1016/j.polymer.2009.06.038>.
- [16] Y. Liu, Y. Peng, J. Luo, J. Liu, X. Liu, *Ind. Eng. Chem. Res.* **2020**, 59(26), 12085–12095. <https://doi.org/10.1021/acs.iecr.0c01300>.
- [17] H. Srinivasan, P. Saravanan, P. Madesh, *Polym. Bull.* **2024**, 81(1), 887–907. <https://doi.org/10.1007/s00289-023-04745-1>.
- [18] S. Mukherjee, B. Lochab, *Chem. Commun.* **2022**, 58(22), 3609–3612. <https://doi.org/10.1039/D2CC00043A>.
- [19] H. Yee Low, H. Ishida, *Polymer* **1999**, 40(15), 4365–4376. [https://doi.org/10.1016/S0032-3861\(98\)00656-9](https://doi.org/10.1016/S0032-3861(98)00656-9).
- [20] N. K. Sini, J. Bijwe, I. K. Varma, *J. Polym. Sci. Part A* **2014**, 52(1), 7–11. <https://doi.org/10.1002/pola.26981>.
- [21] M. C. Aversa, P. Giannetto, C. Caristi, A. Ferlazzo, *J. Chem. Soc. Chem. Commun.* **1982**, 8, 469–470. <https://doi.org/10.1039/C39820000469>.
- [22] O. Vozdvizhenskaya, V. L. Andronova, G. Galegov, G. L. Levit, V. P. Krasnov, V. N. Charushin, *Chem. Heterocycl. Compd.* **2021**, 57(4), 490–497. <https://doi.org/10.1007/s10593-021-02929-z>.
- [23] H. Kanatomi, I. Murase, *Bull. Chem. Soc. Jpn.* **1970**, 43(1), 226–231. <https://doi.org/10.1246/bcsj.43.226>.
- [24] A. R. Katritzky, Y.-J. Xu, R. Jain, *J. Org. Chem.* **2002**, 67(23), 8234–8236. <https://doi.org/10.1021/jo020176e>.
- [25] J. R. Oliveira, D. B. de Freitas, J. F. R. de Oliveira, G. Mele, S. E. Mazzetto, D. Lomonaco, *Eur. Polym. J.* **2021**, 156, 110596. <https://doi.org/10.1016/j.eurpolymj.2021.110596>.
- [26] Y. Deng, Q. Zhang, H. Zhang, C. Zhang, W. Wang, Y. Gu, *Ind. Eng. Chem. Res.* **2014**, 53(5), 1933–1939. <https://doi.org/10.1021/ie402978.s>.
- [27] S. Mukherjee, N. Amarnath, B. Lochab, *Macromolecules* **2021**, 54(21), 10001–10016. <https://doi.org/10.1021/acs.macromol.1c01582>.
- [28] J. Liu, L. Zhang, X. Zhu, Q. Chen, K. Zhang, X. Liu, *ACS Appl. Polym. Mater.* **2023**, 5(8), 6595–6606. <https://doi.org/10.1021/acsapm.3c01107>.
- [29] Chen Qian, Ren Dayong, K. Z. Weichen Sheng, *J. Appl. Polym. Sci.* **2024**, 141(2), 1–10. <https://doi.org/10.1002/app.54792>.
- [30] Ian C. Chagunda, Tiago Fisher, Makenna Schierling, J. S. M. Poisonous Truth *Organometallics* **2023**, 42(19), 2938–2945.
- [31] C. Killeen, J. Liu, H. S. Zijlstra, F. Maass, J. Piers, R. Adams, *Catal. Sci. Technol.* **2023**, 14(13), 4000–4008.
- [32] A. Ray, T. Bristow, C. Whitmore, J. Mosely, *Mass Spectrom. Rev.* **2018**, 37(4), 565–579. <https://doi.org/10.1002/mas.21539>.
- [33] I. Omari, P. Randhawa, J. Randhawa, J. Yu, J. S. McIndoe, *J. Am. Soc. Mass Spectrom.* **2019**, 30(9), 1750–1757. <https://doi.org/10.1007/s13361-019-02252-0>.
- [34] A. Joshi, H. S. Zijlstra, E. Liles, C. Concepcion, M. Linolahti, J. S. McIndoe, *Chem. Sci.* **2021**, 12(2), 546–551. <https://doi.org/10.1039/d0sc05075j>.
- [35] T. C. Penna, G. Cervi, A. F. Rodrigues-Oliveira, B. D. Yamada, R. Z. C. Lima, J. J. Menegon, E. L. Bastos, T. C. Correra, *Rapid Commun. Mass Spectrom.* **2020**, 34(53), 8635. <https://doi.org/10.1002/rcm.8635>.
- [36] M. J. Frisch, G. W. Trucks, H. B. Schlegel, G. E. Scuseria, M. A. Robb, J. R. Cheeseman, G. Scalmani, V. Barone, B. Mennucci, G. A. Petersson, H. Nakatsuji, M. Caricato, X. Li, H. P. Hratchian, A. F. Izmaylov, J. Bloino, G. Zheng, J. L. Sonnenberg, M. Hada, M. Ehara, K. Toyota, R. Fukuda, J. Hasegawa, M. Ishida, T. Nakajima, Y. Honda, O. Kitao, H. Nakai, T. Vreven, J. A. Montgomery, J. E. Peralta, F. Ogliaro, M. Bearpark, J. J. Heyd, E. Brothers, K. N. Kudin, V. N. Staroverov, T. Keith, R. Kobayashi, J. Normand, K. Raghavachari, A. Rendell, J. C. Burant, S. S. Iyengar, J. Tomasi, M. Cossi, N. Rega, J. M. Millam, M. Klene, J. E. Knox, J. B. Cross, V. Bakken, C. Adamo, J. Jaramillo, R. Gomperts, R. E. Stratmann, O. Yazyev, A. J. Austin, R. Cammi, C. Pomelli, J. W. Ochterski, R. L. Martin, K. Morokuma, V. G. Zakrzewski, G. A. Voth, P. Salvador, J. J. Dannenberg, S. Dapprich, A. D. Daniels, Ö. Farkas, J. B. Foresman, J. V. Ortiz, J. Cioslowski, D. J. Fox, *Gaussian 09, Revision D.01*, **2013**.
- [37] A. Lagutschenkov, J. Langer, G. Berden, J. Oomens, O. Dopfer, *Phys. Chem. Chem. Phys.* **2011**, 13(7), 2815–2823. <https://doi.org/10.1039/C0CP02133D>.
- [38] Y. Ulas, *J. Comput. Biophys. Chem.* **2021**, 20(3), 323–335. <https://doi.org/10.1142/s2737416521500150>.
- [39] H. Gümüş, N. Tekin, Y. S. Kara, *J. Appl. Spectrosc.* **2023**, 89(6), 1150–1157. <https://doi.org/10.1007/s10812-023-01481-2>.
- [40] A. F. Rodrigues-Oliveira, F. W. M. Ribeiro, G. Cervi, C. T. Correra, *ACS Omega* **2018**, 3(8), 9075–9085. <https://doi.org/10.1021/acsomega.8b00815>.
- [41] D. Russell, Johnson III. *NIST Computational Chemistry Comparison and Benchmark Database* 101.
- [42] R. S. Galeano Carrano, P. F. Provasi, M. B. Ferraro, I. Alkorta, J. Elguero, S. P. A. Sauer, *ChemPhysChem* **2021**, 22(8), 764–774. <https://doi.org/10.1002/cphc.202001010>.
- [43] R. Isomers, M. Crescentini, S. M. Stow, J. G. Forsythe, J. C. May, J. A. Mclean, D. M. Hercules, *Anal. Chem.* **2018**, 90(24), 14453–14461. <https://doi.org/10.1021/acs.analchem.8b04103>.
- [44] E. Honarvar, A. R. Venter, *J. Am. Soc. Mass Spectrom.* **2018**, 29(12), 2443–2455. <https://doi.org/10.1007/s13361-018-2058-z>.
- [45] A. Krueve, K. Kaupmees, *J. Am. Soc. Mass Spectrom.* **2017**, 28(5), 887–894. <https://doi.org/10.1007/s13361-017-1626-y>.
- [46] C. Y. Wang, H. Q. Li, L. G. Wang, Y. Cao, H. T. Liu, Y. Zhang, *Chin. Chem. Lett.* **2012**, 23(11), 1254–1258. <https://doi.org/10.1016/j.ccl.2012.10.001>.
- [47] R. Zsanett Boros, László Farkas, Károly Nehéz, M. S. Béla Viskolcz, *Polymers (Basel)* **2019**, 11(3), 1–14. <https://doi.org/10.3390/polym11030398>.
- [48] F. W. M. Ribeiro, I. Omari, G. T. Thomas, M. Paul, P. J. H. Williams, J. S. McIndoe, T. C. Correra, *Macromol. Rapid Commun.* **2024**, 45(2), 1–7. <https://doi.org/10.1002/marc.202300470>.
- [49] A. B. Miltojevic, R. D. Vukic, N. S. Radulovic, *Comptes Rendus Chim.* **2013**, 16(3), 257–270. <https://doi.org/10.1016/j.crci.2013.01.010>.
- [50] S. Chirachanchai, S. Phongtamrug, A. Laobuthee, K. Tashiro, *Handbook of Benzoxazine Resins*; Elsevier, **2011**, 111–126. <https://doi.org/10.1016/B978-0-444-53790-4.00049-7>.
- [51] J. Sun, W. Wei, Y. Xu, J. Qu, X. Liu, T. Endo, *RSC Adv.* **2015**, 5(25), 19048–19057. <https://doi.org/10.1039/C4RA16582A>.

Manuscript received: March 15, 2024
Revised manuscript received: June 10, 2024
Accepted manuscript online: June 11, 2024
Version of record online: July 30, 2024